*Articles*

# Binding of $La^{3+}$ to Calmodulin and Its Effects on the Interaction between Calmodulin and Calmodulin Binding Peptide, Polistes Mastoparan†

Jian Hu,‡ Xin Jia,*,§ Qin Li,§ Xiaoda Yang,*,‡ and Kui Wang‡,§

*Department of Chemical Biology, School of Pharmaceutical Sciences and National Research Laboratories of Natural and Biomimetic Drugs, Peking University, Beijing 100083, P. R. China*

*Received October 3, 2003; Revised Manuscript Received December 24, 2003*

ABSTRACT: Binding of $La^{3+}$ to calmodulin (CaM) and its effects on the complexes of CaM and CaM-binding peptide, polistes mastoparan (Mas), were investigated by nuclear magnetic resonance (NMR) spectroscopy, fluorescence and circular dichroism spectroscopy, and by the fluorescence stopped-flow method. The four binding sites of $La^{3+}$ on CaM were identified as the same as the binding sites of $Ca^{2+}$ on CaM through NMR titration of $La^{3+}$ to uniformly $^{15}N$-labeled CaM. $La^{3+}$ showed a slightly higher affinity to the binding sites on the N-terminal domain of CaM than that to the C-terminal. Large differences between the $^{1}H$-$^{15}N$ heteronuclear single quantum coherence (HSQC) spectra of $Ca_4$CaM and $La_4$CaM suggest conformational differences between the two complexes. Fluorescence and CD spectra also exhibited structural differences. In the presence of $Ca^{2+}$ and $La^{3+}$, a hybrid complex, $Ca_2La_2$CaM, was formed, and the binding of $La^{3+}$ to the N-terminal domain of CaM seemed preferable over binding to the C-terminal domain. Through fluorescence titration, it was shown that $La_4$CaM and $Ca_2La_2$CaM had similar affinities to Mas as $Ca_4$CaM. Fluorescence stopped-flow experiments showed that the dissociation rate of $La^{3+}$ from the C-terminal domain of CaM was higher than that from the N-terminal. However, in the presence of Mas, the dissociation rate of $La^{3+}$ decreased and the dissociation processes from both global domains were indistinguishable. In addition, compared with the case of $Ca_4$CaM−Mas, the slower dissociations of Mas from $La_4$CaM−Mas and $Ca_2La_2$CaM−Mas complexes indicate that in the presence of $La^{3+}$, the CaM−Mas complex became kinetically inert. A possible role of $La^{3+}$ in the $Ca^{2+}$−CaM-dependent pathway is discussed.

Lanthanides (Ln)[1] have been known for their diversity in biological effects (*1*), and the application of lanthanides in medicine has high potential (*2*). It was shown that lanthanum chloride inhibited the development of arteriosclerosis on monkeys fed with cholesterol (*3*) and gadolinium chloride attenuated inflammation responses mediated by Kupffer cells (*4*, *5*). The physiological effects of lanthanides related to their profound effects on cell proliferation and apoptosis are also of particular interest and medical significance (*6*−*12*). In agriculture, lanthanides have been used to increase the production of crops and to promote the growth of livestock in China for many years. By applying a mixture of lanthanides nitrate (lanthanum is one of the major components) as an additive to fertilizer or animal food, the levels of lanthanides in organisms of plants and animals were increased to stimulate growth (*6*).

The molecular mechanism of the biological effects of lanthanides is not totally understood so far. It has been considered that lanthanides may play a role in biological functions involving calcium due to the similarity in coordination chemistry between the lanthanides and calcium ion. Calmodulin, a key molecule in the calcium-dependent signal transduction pathway, is of great interest as a potential target of Ln.

Calmodulin (CaM) is a ubiquitous, small calcium-binding protein found in almost all eukaryotic cells and is responsible for converting the intracellular $Ca^{2+}$ signal into a wide range of physiological events. More than 40 proteins were found to be regulated by CaM, including many important enzymes related to protein phosphorylation/dephosphorylation, production of nitric oxide, and motility of the cell (*13*, *14*).

On the basis of structures of both calcium-saturated CaM and *apo*CaM determined by X-ray crystallography and NMR spectroscopy (*15*, *16*), the mechanism of CaM regulation by

† This work was supported by National Natural Science Foundation of China (No. 20101001).

* To whom correspondence should be addressed. Telephone: +86-010-8280-1539, Fax: +86-010-6601-5584, E-Mail: xyang@bjmu.edu.cn. and xjia3988@yahoo.com.

‡ Department of Chemical Biology, School of Pharmaceutical Sciences.

§ National Research Laboratories of Natural and Biomimetic Drugs.

[1] Abbreviations: CaM, calmodulin; NMR, nuclear magnetic resonance; HSQC, heteronuclear single quantum coherence; Mas, polistes mastoparan; CD, circular dichroism; Ln, lanthanides; CaMBP, calmodulin binding protein; Quin 2, 8-amino-2-[(2-amino- 5-methylphenoxy)-methyl]-6-methoxyquinoline-*N*,*N*,*N*′,*N*′-tetraacetic acid; EGTA, ethylene glycol bis(β-aminoethyl ether)-*N*,*N*,*N*′*N*′-tetraacetic acid.

10.1021/bi035784i CCC: $27.50 
Published on Web 02/20/2004

$Ca^{2+}$ has been elucidated (*17*). $Ca^{2+}$ binds to four sites on *apo*CaM in a stepwise manner (*18*). In a cooperation pattern, two $Ca^{2+}$ ions bind to two sites on the C-terminal domain of CaM more tightly, while the other two $Ca^{2+}$ ions bind to the N-terminal domain of the protein less tightly. However, the binding of $Ca^{2+}$ starts from the N-terminal domain (*19*). In the presence of CaM-binding proteins (CaMBPs), the calcium binding to both domains of CaM is in a cooperation way, which makes CaM sensitive to the $Ca^{2+}$ concentration in a narrow range (*20*). The structure of *apo*CaM shows that the two α-helices in each of the "E-F hand" motifs are nearly antiparallel so that the hydrophobic pocket in each of the global domains is closed. Upon $Ca^{2+}$ binding, the two helices become almost perpendicular and the hydrophobic pocket is open, which facilitates the molecular recognition between CaM and CaMBP.

Since CaM can be regarded as an on/off switch regulated by intracellular $Ca^{2+}$, it is conceivable that the biological effects of lanthanides may, at least partially, result from the interaction of lanthanides and CaM. Many results have been reported concerning the effects of lanthanides on CaM. Using laser-induced $Eu^{3+}$ and $Tb^{3+}$ luminescence, it was found that lanthanides could bind to CaM with high affinity, and the binding sites were suggested to be the same as the four calcium-binding sites (*21*, *22*). $Eu^{3+}$ and $Tb^{3+}$ were also believed to bind first to the N-terminal of CaM (*22*, *23*). Recently, through $^1H$-$^{15}N$ heteronuclear single quantum coherence (HSQC) titration, $Yb^{3+}$ was reported to have higher affinity to the N-terminal domain of CaM than $Ca^{2+}$, while its affinity to the C-terminal domain of CaM was comparable with that of $Ca^{2+}$ (*24*). As to the binding preference of $La^{3+}$ among its binding sites on CaM, different results had been reported (*25*, *26*). In addition, the binding properties of different lanthanides to CaM were different from one to another according to Buccigross (*27*). The structures of the N-terminal domain of CaM with two $Ce^{3+}$ ions bound and with two $Ca^{2+}$ ions bound were compared, which revealed that they were essentially similar in topology, and the structure with two $Ce^{3+}$ ions bound was tighter in the core (*28*). The effects of lanthanides on activation of CaM-dependent enzymes had also been investigated, and it was found that Ln activated CaM-dependent enzymes at low concentration while it inhibited them at high concentration (*29*−*31*), but the mechanism is not clear.

Although $La^{3+}$ is one of the closest lanthanides to calcium in coordination chemistry, the interaction of lanthanum and CaM was not studied as much as $Eu^{3+}$ and $Tb^{3+}$ because $La^{3+}$ does not have measurable optical and magnetic properties. In the present study, the binding of lanthanum ion to CaM and its effects on the interaction between CaM and a CaM-binding peptide, polistes mastoparan (Mas), were investigated by nuclear magnetic resonance (NMR) spectroscopy and other spectroscopic methods. The kinetic properties of La/Ca−CaM and La/Ca−CaM−Mas complexes were studied by the fluorescence stopped-flow method. Our results indicate that $La^{3+}$ binds to $Ca^{2+}$-binding sites of CaM, results in different conformation from that of $Ca_4$CaM, and affects the interaction between CaM and Mas.

## MATERIALS AND METHODS

*Materials*. Lanthanum chloride solution was prepared by dissolving $La_2O_3$ (purity 99.99%) in concentrated HCl. After the excess HCl was removed by heating, $LaCl_3$ was redissolved in a 1 mM HCl solution. The stock solution of $LaCl_3$ was diluted into the desired concentration with the NMR buffer or the fluorescence buffer immediately before use. Polistes mastoparan (VNWKKIGQHILSV) was purchased from Sigma without further purification. Quin 2, a $Ca^{2+}$ fluorescence probe, was also from Sigma. All other chemicals used were of analytical grade.

The NMR buffer contains 5 mM Pipes, 100 mM KCl, and 0.01% sodium azide and was adjusted to pH 6.5; the fluorescence buffer contains 20 mM Hepes, 100 mM KCl, and 0.02% sodium azide, and was adjusted to pH 7.0. All solutions were passed through a Chelex 100 (Sigma) column to remove trace amounts of $Ca^{2+}$ and other high valence metal ions.

*Preparation of $^{15}N$-Labeled and Nonlabeled apoCaM*. *Escherichia coli* JM109 (DE3) harboring a plasmid containing the chicken calmodulin gene (generous gift from Dr. T. Squier at University of Kansas) was grown on minimal medium (M9) containing $^{15}NH_4Cl$ (99%, Isotec Inc.) as the sole nitrogen source. CaM was isolated and purified by affinity chromatography on phenyl-Sepharose, followed by anion exchange chromatography on QAE-Sepharose. The homogeneity was checked by SDS−PAGE.

The purified CaM was concentrated to about 30 mg/mL through ultrafiltration in a solution containing 20 mM Hepes, 100 mM KCl, and 2 mM EGTA at pH 7.0 and then passed through a Sephadex G-25 column (Pharmacia PD10) preequilibrated and eluted with the NMR buffer. The concentration of the protein was determined by measuring absorption at 276 nm ($\epsilon_{276} = 3300\ M^{-1}\ cm^{-1}$ (*32*)).

The nonlabeled *apo*CaM was prepared in the same way described above except that *apo*CaM was eluted with the fluorescence buffer.

*NMR Titration of $La^{3+}$ to CaM*. The concentration of $^{15}N$-labeled *apo*CaM was 0.9 mM in 90% NMR buffer/10% $D_2O$. During the titration, a small volume of 22.5 mM $La^{3+}$ in the NMR buffer was titrated into CaM solution, and $^1H$-$^{15}N$ HSQC spectra were recorded on a Bruker AV 500 NMR spectrometer equipped with a cryoprobe at 296 K. For the titration of $La^{3+}$ to $Ca^{2+}$-semisaturated or $Ca^{2+}$-saturated CaM, all procedures were the same, except that 2 or 5 equiv of $Ca^{2+}$ was added to *apo*CaM before the titration and the HSQC spectra were recorded on a Varian INOVA 500 NMR spectrometer. The NMR data were processed and analyzed using Felix 2000 software package (Accelrys, Inc.) on an SGI Indigo workstation.

*Fluorescence Titration*. All fluorescence titration experiments were performed on a RF-5301 fluorometer at room temperature. *apo*CaM was diluted to 5 μM with the fluorescence buffer and aliquots of metal ions were added to the desired concentration. The intrinsic fluorescence of CaM was measured at $\lambda = 307$ nm with the excitation at 273 nm (both slit widths were 5 nm).

Mas was dissolved in the fluorescence buffer to the concentration of 2 μM. CaM containing different amounts of metal ions was titrated into the Mas solution. The samples were excited at 290 nm to measure the fluorescence of tryptophan (Trp) of Mas and the emission spectra were recorded in the range from 310 to 400 nm. An excitation slit width of 3 nm was used to reduce the possible interference from CaM intrinsic fluorescence. The binding

process of CaM to Mas was monitored with the fluorescent emission at 325 nm with the slit width of 10 nm.

*Kinetic Properties of La/Ca−CaM and La/Ca−CaM−Mas Complexes.* The kinetic properties of La/Ca−CaM and La/Ca−CaM−Mas were investigated using a Cary Eclipse fluorescence spectrometer with a SPF-20 hand-driven stopped-flow accessory at room temperature. The dead time of the system was estimated as 50 ms. All stopped-flow experiments were performed in the fluorescence buffer. The protein solution containing La/Ca−CaM or La/Ca−CaM−Mas complexes (the concentration of CaM was 5 $\mu$M) and the chelator solution containing 10 mM EGTA or 100 $\mu$M Quin 2 were mixed using two manual syringe pumps.

The release of $Ca^{2+}$ from CaM was monitored according to the increase fluorescence intensity of Quin 2, upon the formation of $Ca^{2+}$-Quin 2, excited at 336 nm with slit width of 2.5 nm. The release of $Ca^{2+}$ or $La^{3+}$ was also monitored according to the decrease in fluorescence intensity of Quin 2 excited at 366 nm with a slit width of 5 nm. The fluorescence of Quin2 was recorded at 490 nm. The release of Mas from CaM−Mas complexes induced by EGTA was monitored according to the changes of fluorescence of Trp of Mas at 325 nm using the same instrumental parameters mentioned in the fluorescence titration experiments. All data points were recorded with an interval of 12.5 ms and repeated at least four times. The kinetic parameters were obtained by fitting the data to monophasic or biphasic model using a Microcal ORIGIN program.

*Circular Dichroism Spectra of La/Ca−CaM and La/Ca−CaM−Mas Complexes*. The final concentration of CaM or CaM−Mas (in a ratio 1:1) was 10 $\mu$M in 5 mM Tris-HCl at pH 7.5. The circular dichroism spectra were recorded in the wavelength range of 200−250 nm in a 0.2-cm path length cuvette on a JASCO J-715 spectrometer at room temperature. At least four scans were performed for each spectrum and the baseline was subtracted. The CD spectra are presented as mean residue ellipticity weight, e.g., $[\theta]$ (deg cm$^2$ mol$^{-1}$). The contents of secondary structures were estimated by data fitting using a CONTINLL program in the CDPro software package.

## RESULTS

*Binding of $La^{3+}$ to apoCaM*. $La^{3+}$ was titrated into $^{15}$N-labeled *apo*CaM, and HSQC spectra were recorded at each titration. The HSQC spectra of *apo*CaM and $Ca^{2+}$-saturated CaM are shown in Figure 1A,B, in which the complete backbone assignments are based on the published data (*33*−*35*).

The HSQC spectra changed dramatically with the addition of $La^{3+}$ to *apo*CaM. As shown in Figure 1C−F, a few new cross-peaks appeared when the ratio of $La^{3+}$ to CaM was 0.5 and more new cross-peaks emerged with the increase of $La^{3+}$/CaM ratio. At the same time, the intensities of the original cross-peaks of *apo*CaM decreased for most residues and disappeared finally.

The binding of $La^{3+}$ to *apo*CaM reduces *apo*CaM signal intensities on HSQC spectra differently among residues. Figure 2 shows the quantitative plots of the normalized signal intensities versus the residue number for samples with $La^{3+}$/CaM molar ratios of 0.5, 1, and 2. In comparison with other residues, larger decreases of signal intensities were observed in four segments corresponding to residues 19−35, 53−70, 88−102, and 128−139, which constitute the four binding sites I−IV of $Ca^{2+}$ on CaM (*15*). By looking closely, it can be found that the binding of $La^{3+}$ has different preferences between the two global domains of CaM. When the first 0.5 equiv of $La^{3+}$ was added to *apo*CaM, those residues at sites I and II (the N-terminal binding sites) underwent larger intensity decreases than those at sites III and IV (the C-terminal binding sites), although the signal intensities of nearly all residues decreased (Figure 2). When the next 0.5 equiv of $La^{3+}$ was added, the binding at site III and site IV was observed. The $La^{3+}$ binding at the C-terminal was not as explicit as at the N-terminal until the $La^{3+}$/CaM molar ratio reached 2. This result suggests that $La^{3+}$ prefers binding to the N-terminal domain over the C-terminal. It also clearly reveals a cooperative pattern for binding of $La^{3+}$ in each of the global domains, which is similar to the binding of $Ca^{2+}$ (*18*).

It can be seen in Figure 1B,F that the HSQC spectra of $La_4$CaM and $Ca_4$CaM are quite different. If superimposing the two spectra, only a few cross-peaks can be overlapped, the majority of which are in fact from the amino acid residues at the two ends of the protein. The chemical shift changes were observed not only for the residues near the metal ions binding sites but also for those far away from these sites.

The fluorescence titration curves of *apo*CaM by $Ca^{2+}$ and $La^{3+}$ are shown in Figure 3A. It can be seen that although binding of $La^{3+}$ on *apo*CaM increases the intrinsic fluorescence of CaM as $Ca^{2+}$ does, the shape of $La^{3+}$ titration curve and the degree of fluorescence increase are different from those of $Ca^{2+}$. When the $La^{3+}$/CaM ratio was over 4, the intrinsic fluorescence started to decrease, indicating that nonspecific binding of $La^{3+}$ to CaM may take place.

The CD spectra of $Ca_4$CaM and $La_4$CaM are shown in Figure 3B. It is shown that binding of either $Ca^{2+}$ or $La^{3+}$ induces secondary structure changes characterized by an increase of α-helix content (from 41 to 51% for $Ca^{2+}$ and from 41 to 52% for $La^{3+}$). The differences on the secondary structures of the two complexes do not seem large.

*Binding of $La^{3+}$ to $Ca^{2+}$−CaM and Formation of Hybrid Complex, $Ca_2La_2$CaM*. Figure 4A,B shows the HSQC spectra of $Ca_2$CaM and $Ca_2$CaM after addition of 2 equiv of $La^{3+}$. It is observed that, for most of the signals in Figure 4B corresponding to the $Ca^{2+}$-saturated C-terminal residues (labeled in Figure 4A), there is no change of chemical shift or decrease of signal intensity. In comparison with the HSQC spectrum of $La_4$CaM (Figure 1F), many new signals in Figure 4B can be found in the spectrum of $La_4$CaM. This result suggests the formation of a hybrid complex, $Ca_2La_2$CaM with $Ca^{2+}$ binding on the C-terminal domain and $La^{3+}$ binding on the N-terminal domain. As the ratio of $La^{3+}$ to $Ca^{2+}$ increased to 5:2, the aggregation of protein could be observed and the intensities of most cross-peaks decreased dramatically (data not shown).

When 2.5 mol of $La^{3+}$ were added to $Ca^{2+}$-saturated CaM (5 equiv of $Ca^{2+}$ was added to *apo*CaM before $La^{3+}$ titration to guarantee $Ca^{2+}$ saturation), the resulting HSQC spectrum (Figure 4C) can be found almost identical to that of $Ca_2La_2$-CaM (Figure 4B). Figure 5 shows the decrease of NMR signal intensities of each residue in the four $Ca^{2+}$-binding sites during the titration of $La^{3+}$ to $Ca_4$CaM. The signal intensities of the residues at site I and II decreased dramati-

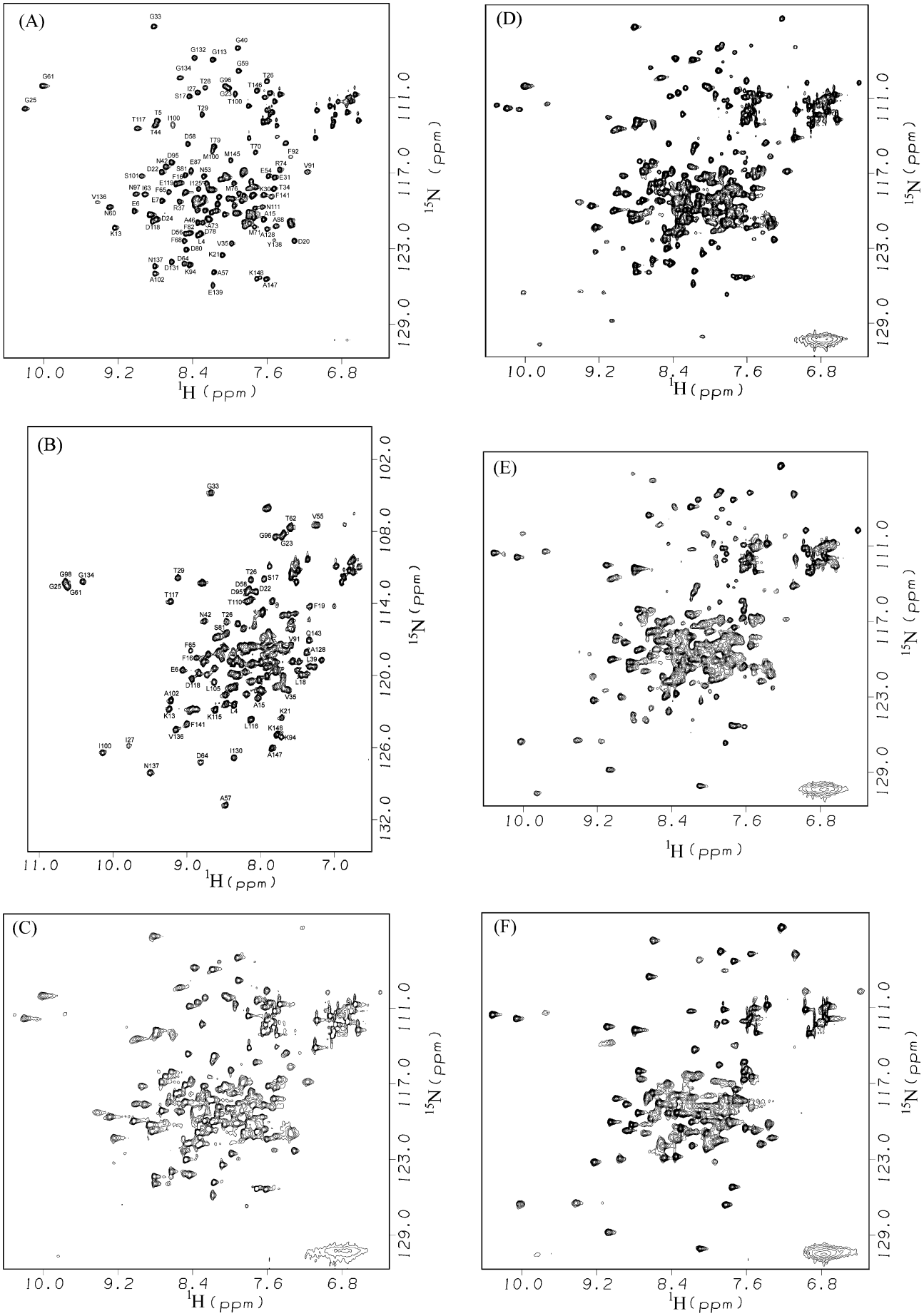


FIGURE 1: $^1$H-$^{15}$N HSQC spectra of uniformly $^{15}$N-labeled calmodulin (0.9 mM in the NMR buffer) with different concentrations of metal ions. (A) *apo*CaM; (B) $Ca_4$CaM; (C−F) calmodulin with 0.5, 1, 2, and 4 equiv of $La^{3+}$, respectively.

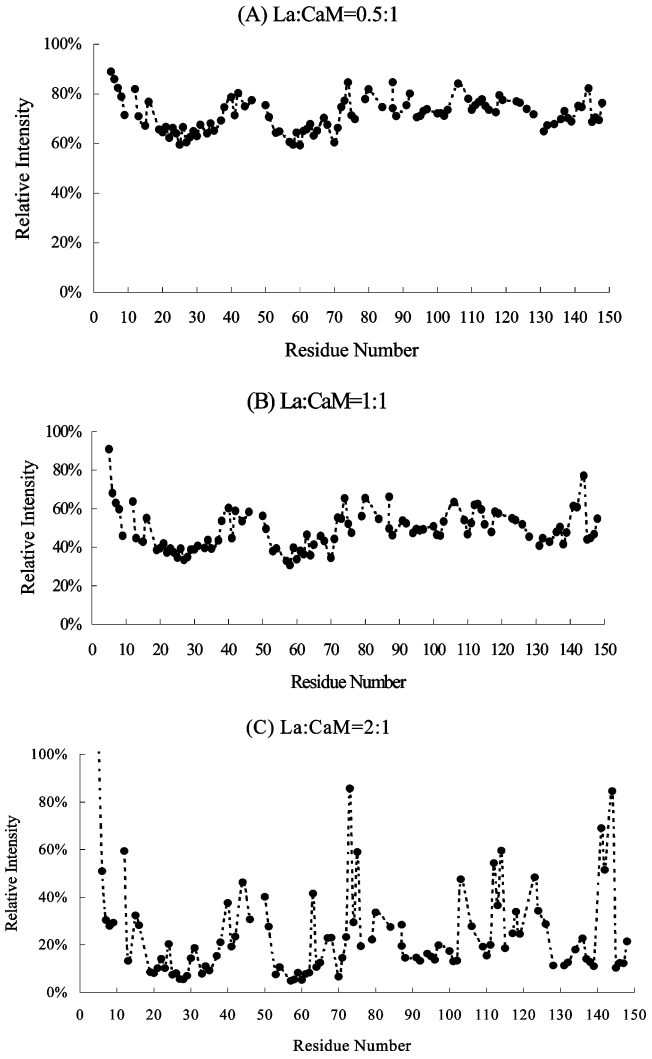


FIGURE 2: The changes of cross-peak height of each residue of *apo*CaM during the titration of $La^{3+}$ to *apo*CaM. (A−C) Calmodulin with 0.5, 1, and 2 equiv of $La^{3+}$, respectively. All cross-peak heights were normalized based on the initial cross-peak height of each residue. Some residues are not included due to overlapping of the signals.

cally with addition of the first 2 equiv of $La^{3+}$, while those at site III and IV only decreased slightly until the ratio of $La^{3+}$/CaM was over 2, and they began to decrease significantly. The result suggests that $La^{3+}$ preferably replaces $Ca^{2+}$ at site I and II (the N-terminal). Similar observation was reported recently in the substitution of $Ca^{2+}$ on CaM by $Yb^{3+}$ (*24*).

Figure 6 illustrates typical changes of HSQC signals along the process of $Ca^{2+}$ substitution by $La^{3+}$. With addition of $La^{3+}$, the signal intensity of G61, which is a representative residue on the site II, decreased gradually until it disappeared when the La/CaCaM ratio was 2.5. On the other hand, the cross-peaks of G98 and G134, representing residues on site III and IV, respectively, were not affected at the beginning until the La/CaCaM ratio reached 3. Simultaneously, a new cross-peak "A" appeared when the ratio was above 1, reached the maximum intensity with a ratio of La to CaCaM of about 2.5, but gradually disappeared and could not be found in the spectrum of $La_4$CaM. In addition, the cross-peaks "B" and "C" that could be found in the spectrum of $La_4$CaM appeared when the ratio reached 1.5 and their intensities kept increasing during the titration.

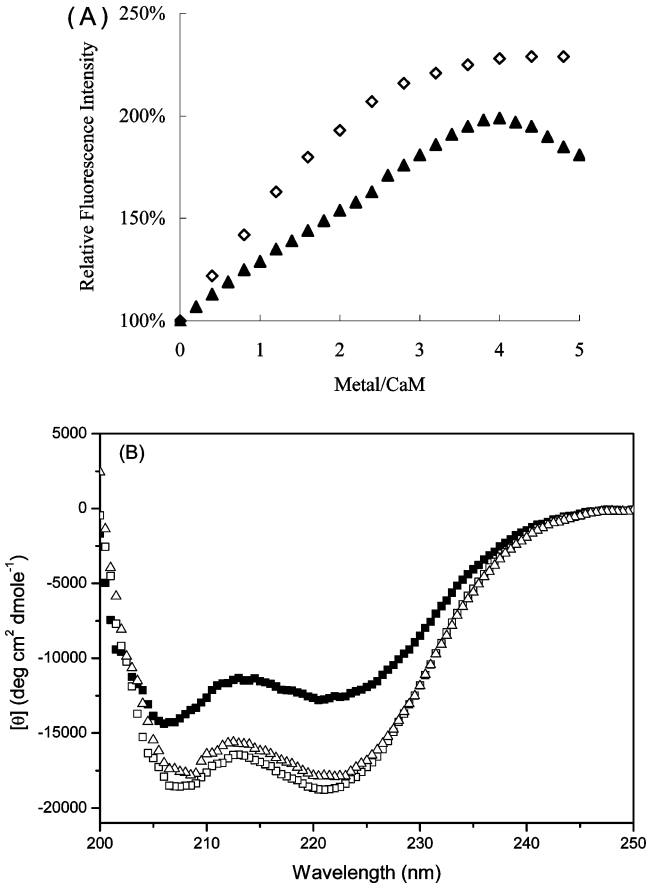


FIGURE 3: (A) Fluorescence titration of $Ca^{2+}$ (◇) and $La^{3+}$ (▲) to *apo*CaM. The concentration of *apo*CaM was 5 $\mu$M in the fluorescence buffer. Aliquots of stock solution of $Ca^{2+}$ or $La^{3+}$ were added. (B) Circular dichroism spectra of *apo*CaM (■), $La_4$CaM (△) and $Ca_4$CaM (□). The concentration of CaM or CaM/Mas (at a molar rate of 1:1) was 10 $\mu$M in 5 mM Tris-HCl, pH 7.5.

*Dissociation of Metal Ions from Metal Ions−CaM Binary Complexes*. The time course of dissociation of metal ions or Mas from metal−CaM or metal−CaM−Mas complexes is shown in Figure 7 and the kinetic parameters calculated are presented in Tables 1 and 2. Dissociation of $La^{3+}$ from $La_4$CaM was investigated with the fluorescence stopped-flow method by monitoring the CaM intrinsic fluorescence changes and the fluorescence changes of the $Ca^{2+}$ probe, Quin 2. The two methods gave consistent results (Table 1) and showed a biphasic process in the dissociation, one faster phase with a rate ($k_f$) of ∼10 $s^{-1}$ and the other slower phase with a rate ($k_s$) of ∼ 1.6 $s^{-1}$. The dissociation rates of $La^{3+}$ from $La_4$CaM were close to that of $Tb^{3+}$ from $Tb_4$CaM as reported (*36*).

The dissociation of $Ca^{2+}$ from $Ca_4$CaM and those of $Ca^{2+}$ and $La^{3+}$ from the hybrid complex, $Ca_2La_2$CaM, were determined by monitoring the changes of fluorescence of Quin 2. The dissociations of $Ca^{2+}$ and $La^{3+}$ from CaM were differentiated according to the different responses of Quin 2 to $Ca^{2+}$ and to $La^{3+}$: when excited at 336 nm, the fluorescence of Quin 2 increased about 10-fold upon $Ca^{2+}$ binding, but decreased about 50% upon $La^{3+}$ binding (data not shown). The results listed in Table 1 show that $Ca^{2+}$ released from $Ca_4$CaM with a rate of ∼8 $s^{-1}$, consistent with the dissociation rate of $Ca^{2+}$ from the C-terminal of CaM reported previously (*37*), while the dissociation rate from the N-terminal was too large (∼700 $s^{-1}$ ) (*37*) to be detected

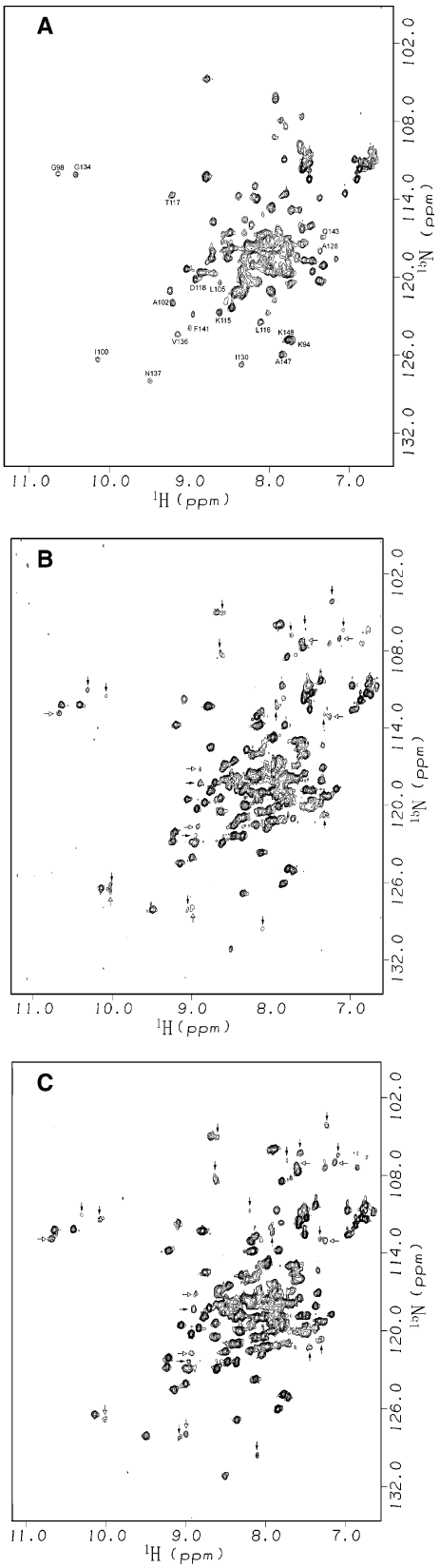


FIGURE 4: $^1$H-$^{15}$N HSQC spectra of CaM with different concentrations of $Ca^{2+}$ and $La^{3+}$. (A) CaM with 2 equiv of $Ca^{2+}$. (B) CaM with 2 equiv of $Ca^{2+}$ and 2 equiv of $La^{3+}$. (C) CaM with 5 equiv of $Ca^{2+}$ and 2.5 equiv of $La^{3+}$. The arrows in (B) and (C) indicate some new cross-peaks compared with the spectrum of $Ca_2$CaM (A). The solid arrows indicate the peaks could be found in the spectrum of $La_4$CaM, and the open arrows indicate the transitional signals whose signal intensities decreased when the La/CaCaM molar ratio was over 2 or 2.5.

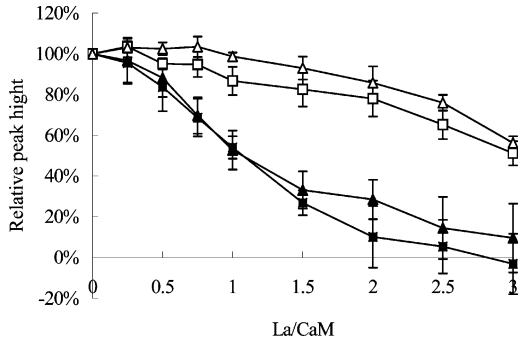


FIGURE 5: Titration curves of the four $Ca^{2+}$ binding sites when $La^{3+}$ was titrated into $Ca_4$CaM (Ca: CaM = 5:1). Sites I−IV refer to residues 19−35 (■), 55−68 (▲), 95−102 (□), and 128−139 (△), respectively. Means of normalized cross-peak heights inside each binding site are plotted as a function of $La^{3+}$/CaM ratio.

Table 1: Dissociation Kinetics of CaM-Metal Binary System

| system | method[a] | $k_f$ $(s^{-1})$[b] | $k_s$ $(s^{-1})$[b] |
|---|---|---|---|
| $Ca_4$CaM | Quin 2 (336 nm) | NA[c] | $7.82 \pm 0.54$ |
| $La_4$CaM | Quin 2 (366 nm) | $11.8 \pm 0.29$ (0.31)[d] | $1.4 \pm 40.06$ (0.69) |
| | EGTA (307 nm) | $8.60 \pm 0.38$ (0.77)[d] | $1.96 \pm 0.16$ (0.23) |
| $Ca_2La_2$CaM | Quin 2 (336 nm) | $8.14 \pm 0.34$[d,e] | $1.20 \pm 0.37$[e] |

[a] Method shows the chelator used and the detection wavelength in brackets. [b] For biphasic system, dissociation rates of the fast phase and the slow phase are named as $k_f$ and $k_s$ respectively, and the relative amplitude of each phase is in brackets. [c] Not applicable. [d] The amplitude of the fast phase is underestimated due to the dead time of the instrument. [e] The relative amplitude cannot be calculated due to the two opposing and separated phases. The fluorescence change of the increase phase was 35.6, and that of the decrease one was 2.8.

Table 2: Dissociation Kinetics of CaM−Metal−Mas Ternary System

| system | method[a] | $k_f$ $(s^{-1})$[b] | $k_s$ $(s^{-1})$[b] |
|---|---|---|---|
| $Ca_4$CaM−Mas | Quin 2 (336 nm) | $18.1 \pm 0.25$ (0.36)[c] | $1.04 \pm 0.02$ (0.64) |
| | EGTA (325 nm) | $0.91 \pm 0.01$ | |
| $La_4$CaM−Mas | Quin 2 (366 nm) | $0.65 \pm 0.01$ | |
| | EGTA (325 nm) | $0.43 \pm 0.02$ | |
| $Ca_2La_2$CaM−Mas | Quin 2 (366 nm) | $6.05 \pm 0.49$ (0.23) | $0.34 \pm 0.01$ (0.77) |
| | EGTA (325 nm) | $0.30 \pm 0.01$ | |

[a] Method shows the chelator used, and the detection wavelength in brackets. [b] For biphasic system, dissociation rates of the fast phase and the slow phase are named as $k_f$ and $k_s$ respectively, and the relative amplitude of each phase is in brackets. [c] The amplitude of the fast phase is underestimated due to the dead time of the instrument.

due to the limit of instrumental detection. The release of metal ions from the hybrid complexes, $Ca_2La_2$CaM, showed a biphasic process: a faster phase with a large increase in fluorescence and a slower phase with a small fluorescence decrease. Clearly, the faster fluorescence increase is due to the release of $Ca^{2+}$ with $k_f = 8.1\ s^{-1}$, and the slower one should be the release of $La^{3+}$ with $k_s = 1.2\ s^{-1}$. Therefore, it could be deduced that in the case of $La^{3+}$ dissociation from $La_4$CaM the slower process corresponds to the release of $La^{3+}$ from the N-terminal domain of CaM and the faster one is that from the C-terminal.

*Effects of $La^{3+}$ on Binding Affinity of CaM to Mas*. The increase of fluorescence intensity of the unique Trp3 of Mas at 325 nm, along with the decrease at 350 nm, was used to monitor formation of Mas−CaM complexes. The binding

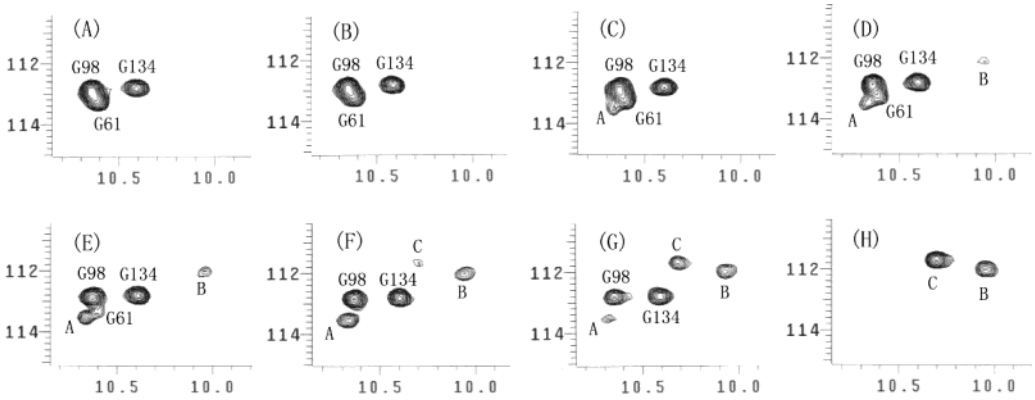


FIGURE 6: Changes of $^{1}H$-$^{15}N$ HSQC spectra in a representative region along the titration of $Ca_4CaM$ (Ca:CaM = 5:1) by $La^{3+}$. The Ca/CaM/La molar ratio from spectrum (A) to (H) is 5:1:0, 5:1:0.5, 5:1:1, 5:1:1.5, 5:1:2, 5:1:2.5, 5:1:3, 0:1:4, respectively. Cross-peaks "A", "B" and "C" represent new signals that emerged during the titration.

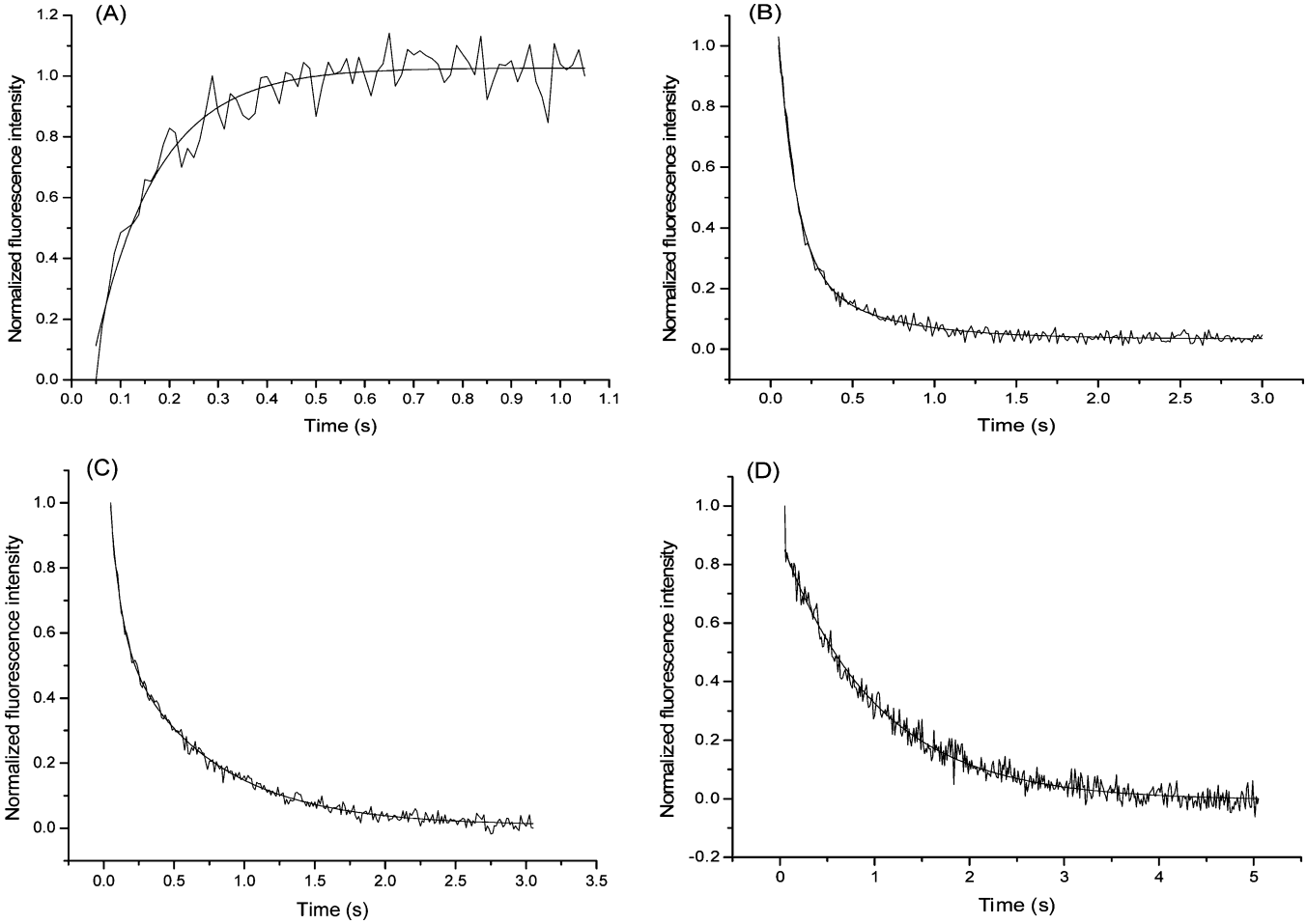


FIGURE 7: Time course of dissociation of metal ions or Mas from metal−CaM complexes or metal−CaM−Mas. (A) The dissociation of $Ca^{2+}$ from $Ca_4CaM$ in the presence of Quin 2 and monitored by excitation at 336 nm. (B) The dissociation of $La^{3+}$ from $La_4CaM$ in the presence of Quin 2 and monitored by excitation at 366 nm. (C) The dissociation of $La^{3+}$ from $La_4CaM$ in the presence of EGTA and monitored by the intrinsic fluorescence of CaM. (D) The dissociation of Mas from the $Ca_4CaM$−Mas complex in the presence of EGTA and monitored by the fluorescence of the unique tryptophan on Mas. Details are described in Materials and Methods.

curves of $Ca_4CaM$, $La_4CaM$, $Ca_2La_2CaM$, and $La_8CaM$ to Mas are shown in Figure 8. It is showed that the binding affinities of $La_4CaM$ ($K_d$ = 180 nM) and $Ca_2La_2CaM$ ($K_d$ = 151 nM) to Mas are close to that of $Ca_4CaM$ ($K_d$ = 119 nM). However, when the molar ratio of $La^{3+}$/CaM is 8, the binding curve of $La_8CaM$ to Mas can be seen to be "right shifted" and the binding affinity largely decreases ($K_d$ = 335 nM).

The fluorescence spectra and CD spectra of $Ca_4CaM$−Mas and $La_4CaM$−Mas are shown in Figure 9. Little differences between the two complexes on both spectra are observed, which indicates the structural similarity between the two complexes.

*Effects of $La^{3+}$ on the Kinetic Properties of CaM−Mas Complexes.* The dissociation rates of Mas and metal ions from CaM−Mas complexes are measured (Figure 7) and

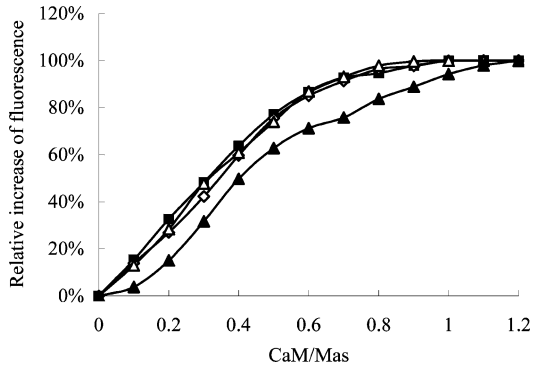


FIGURE 8: Binding curves of $Ca_4$CaM (■), $La_4$CaM (◊), $Ca_2La_2$-CaM (△), and $La_8$CaM (▲) to Mas. Mas, at a concentration of 2 $\mu$M, was titrated by CaM bound with different amounts of metal ions in the fluorescence buffer. The fluorescence of Trp of Mas at 325 nm was recorded and the normalized data are plotted as a function of the molar ratio of CaM/Mas.

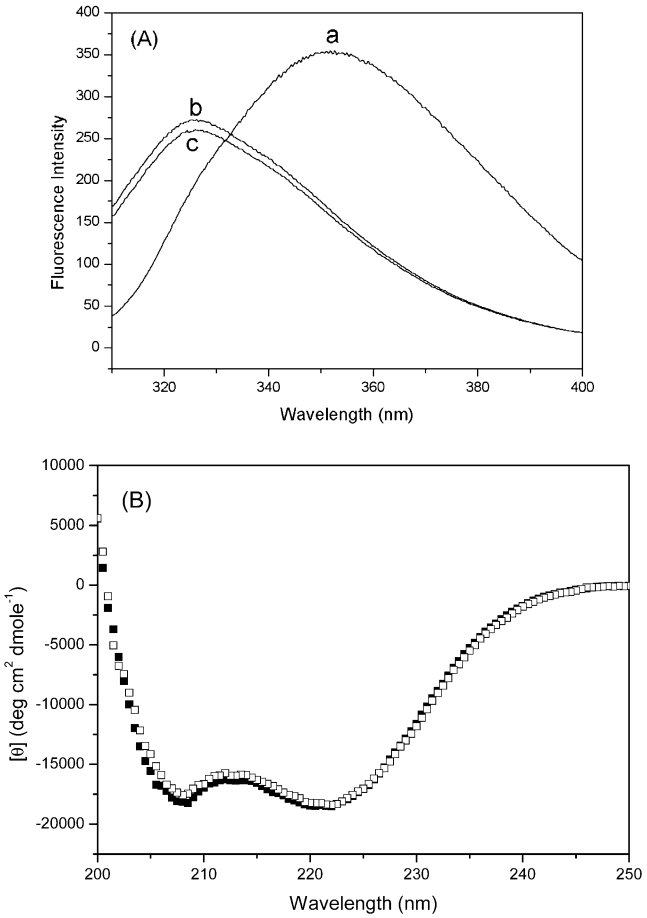


FIGURE 9: (A) Fluorescence spectra of Trp of Mas (a), $Ca_4$CaM−Mas (b), and $La_4$CaM−Mas (c). The concentration of Mas was 4 $\mu$M in the fluorescence buffer. The Trp of Mas was excited at 290 nm (slit width was 3 nm), and the emission spectra were recorded from 310 to 400 nm (slit width was 10 nm). (B) CD spectra of $Ca_4$CaM−Mas (■) and $La_4$CaM−Mas (□). The concentrations of the protein and the peptide were all 10 $\mu$M in 5 mM Tris-HCl, pH 7.5.

summarized in Table 2. Dissociation of $Ca^{2+}$ from CaM−Mas is a biphasic process that is consistent with previous reports (*38*). The dissociation rate of Mas from $Ca_4$CaM−Mas (0.91 $s^{-1}$) is close to that of the slower phase of $Ca^{2+}$ dissociation from $Ca_4$CaM−Mas (1.04 $s^{-1}$).

Dissociation of $La^{3+}$ from the CaM−Mas complex is a monophasic process, so that the dissociations of $La^{3+}$ from the N-terminal and the C-terminal of CaM are unable to be distinguished. The dissociation rate of Mas (0.43 $s^{-1}$) from the $La_4$CaM−Mas complex is close to that of $La^{3+}$ (0.65 $s^{-1}$) and was slower than that from the $Ca_4$CaM−Mas complex (0.91 $s^{-1}$).

Also from Table 2 one can find that for the $Ca_2La_2$CaM−Mas complex the dissociation of the metal ions from CaM−Mas is a biphasic process with slower rates in comparison with the $Ca_4$CaM−Mas complex. The dissociation rate of Mas from the $Ca_2La_2$CaM−Mas complex (0.30 $s^{-1}$) is similar to that of the $La_4$CaM−Mas complex.

## DISCUSSION

*$La^{3+}$ Binds to CaM with Different Binding Preferences between the N- and C-Terminal Domains of CaM.* Our NMR results proved that $La^{3+}$ shares the same binding sites with $Ca^{2+}$ on CaM as predicted. In addition, it was observed that the excess amount of $La^{3+}$ binds to CaM nonspecifically, which is consistent with previous reports. The nonspecific binding of $La^{3+}$ results in (i) disappearance of NMR signals (data not shown) and protein aggregation; (ii) reduced intrinsic fluorescence of CaM (Figure 3); and (iii) decrease of the binding affinity between CaM and Mas (Figure 8).

Different from $Ca^{2+}$, $La^{3+}$ binds to the $Ca^{2+}$ sites with a priority on the N-terminal domain over the C-terminal domain, although the priority is not as large as that of $Tb^{3+}$ (*22*, *23*). The kinetic experiments also suggest such binding preference by showing that the dissociation rate of $La^{3+}$ from the N-terminal of CaM was smaller than that from the C-terminal. This gives different results from some previous reports. Tsai et al. considered that $La^{3+}$, as $Tb^{3+}$ and $Eu^{3+}$, would bind to the N-terminal domain of CaM with high priority (*25*). While Ouyang reported that the site IV was the first binding site of $La^{3+}$, site I and site II were the second and the third, and site III showed the lowest affinity to $La^{3+}$ (*26*). The discrepancy between the observations of Ouyang and us may be reasoned as the following. (i) We labeled all backbone nitrogen, but only those on Gly were labeled in Ouyang's work. (ii) We used a HSQC method that is more sensitive with sharper signals and a better resolution for a protein having a size like CaM than the HMQC method used in Ouyang's study. Since the difference in the binding preference among the binding sites is not so great, the methods used in the studies are very critical.

*Conformation of $La_4$CaM Has Subtle Differences from that of $Ca_4$CaM.* $La^{3+}$ binds to the $Ca^{2+}$ sites of CaM but results in a conformation that is subtly different from that of $Ca_4$CaM. This is supported by the following evidence: (i) the HSQC spectrum of $La_4$CaM was quite different from that of $Ca_4$CaM and the HSQC spectrum is known to be sensitive to the protein's folding; (ii) chemical shift changes were observed for the residues that are far away from the metal binding sites and thus hardly affected by the highly charged $La^{3+}$ ions; and (iii) in the fluorescence titration experiments, the degree of CaM intrinsic fluorescence increase caused by the binding of $La^{3+}$ was smaller than that caused by $Ca^{2+}$ binding. Since CD spectra showed little differences in the contents of secondary structures, the conformational differences between $Ca_4$CaM and $La_4$CaM may be considered in the ternary structure.

*A Hybrid Complex, $Ca_2La_2CaM$, Forms as an Intermediary Species along the Titration of $La^{3+}$ to $Ca_4CaM$.* Formation of the hybrid complex, $Ca_2La_2CaM$, is indicated in comparing HSQC spectra of $Ca_2La_2CaM$ (Figure 4B), $Ca_2CaM$ (Figure 4A), and $La_4CaM$ (Figure 1F). It forms as a main intermediate during the substitution of $Ca^{2+}$ on $Ca_4CaM$ by $La^{3+}$, which was strongly supported by Figures 5 and 6. It could be observed that the signals of residues on site I and site II decreased greatly before the La/CaCaM ratio was 2, but the signals on site III and site IV decreased only after the ratio reached 2. According to this observation, it could be deduced that $La^{3+}$ selectively substitutes $Ca^{2+}$ in N-terminal domain of $Ca_4CaM$ first and the hybrid complex $Ca_2La_2CaM$ has the two $Ca^{2+}$ ions binding at the C-terminal and the two $La^{3+}$ ions at the N-terminal.

*Binding of $La^{3+}$ on CaM Does not Change the Binding Affinity between CaM and Mas, but Makes the CaM−Mas Complex More Kinetically Inert.* Polistes mastoparan is a typical CaM-binding peptide with 14 amino acid residues, and it is frequently used to investigate the molecular recognition process of CaM (*19*, *39*). Although conformational differences may exist among $Ca_4CaM$, $La_4CaM$, and $Ca_2La_2CaM$ in the absence of Mas, the three metal−CaM complexes bind to Mas with similar binding affinities (Figure 6), and the results from the fluorescence and CD studies suggest conformational similarity of $Ca_4CaM$−Mas and $La_4CaM$−Mas complexes (Figure 9).

In the presence of Mas, the higher binding affinity of $Ca^{2+}$ to CaM and the binding cooperation between the two global domains slow the dissociation of $Ca^{2+}$ from the $Ca_4CaM$−Mas complex compared with that from $Ca_4CaM$. The dissociation rate of Mas from the $Ca_4CaM$−Mas complex was close to that of $Ca^{2+}$ from the C-terminal of CaM in the complex. These results support the proposed idea that during the dissociation of the CaM-binding peptide from the CaM−peptide complex, the release of the peptide is associated with the release of $Ca^{2+}$ from the C-terminal of CaM, and the $Ca_2CaM$−peptide complex is an important intermediate species (*38*).

The dissociation rate of $La^{3+}$ from CaM was also found to be reduced in the presence of Mas ($\sim$0.5 $s^{-1}$). This result indicated that the binding affinity of $La^{3+}$ to CaM might increase in this condition, just as that in the case of $Ca^{2+}$. The fact that the disassociation of $La^{3+}$ from $La_4CaM$−Mas complexes became a monophasic process suggests the cooperation effect between the two global domains of CaM is so strong in the $La_4CaM$−Mas complex that the dissociations of $La^{3+}$ from both domains are experimentally beyond distinguishable in kinetics.

Compared with the $Ca_4CaM$−Mas complex, the release rate of Mas from the $La_4CaM$−Mas complex was reduced and close to the dissociation rate of $La^{3+}$ from the $La_4CaM$−Mas complex. The similar result was also found in the case of the $Ca_2La_2CaM$−Mas complex. The inertia of $La^{3+}$ in kinetics can at least partially explain the reduced dissociation rate of Mas from the CaM−Mas complex if the release of metal ions from the CaM−Mas complex is the determination step during the release of Mas. However, the release of a peptide from a CaM−peptide complex may precede the release of metal ions from CaM as pointed by Brown et al. (*38*). The possibility that $La^{3+}$ influences the conformation of CaM−Mas complexes (it should be slight between $Ca_4CaM$−Mas and $La_4CaM$−Mas as suggested by similar fluorescence and CD spectra) and then decreases the release rate of Mas cannot be excluded.

*A Possible Role for $La^{3+}$ in the $Ca^{2+}$−CaM-Dependent Pathway.* Reportedly, lanthanides could be taken up by cells through multiple ways (*40*−*43*) and accumulated there (*44*, *45*). According to the study by Pillai et al., the intracellular concentration of free lanthanum ion ($[La^{3+}]_i$) could be over 80 nM (*46*). Peeters et al. also reported that $La^{3+}$ could enter ventricular cells through $Na^+$−$Ca^{2+}$ exchange and accumulated $\sim$250 nM of free $La^{3+}$ within 1 min upon incubation of the cells with 0.1−1 mM of $La^{3+}$ (*47*). Since $La^{3+}$ binds to CaM with a $K_d$ in the submicromolar scale (*48*), CaM is considered a highly potential target of $La^{3+}$. Likely, $La^{3+}$, after entering the cells, could bind to CaM to form La−CaM or Ca−La−CaM complexes, such as $La_4CaM$, by binding to *apo*CaM, and $Ca_2La_2CaM$ hybrid complexes by binding to the $Ca^{2+}$-saturated or $Ca^{2+}$-semisaturated CaM. Both forms of $La^{3+}$-containing CaM have shown similar affinities to the CaM-binding peptide in the present study. Since most of CaM in the rest cell is believed to be partially saturated by calcium (*49*), the hybrid complex $Ca_2La_2CaM$ may exist as the most likely physiological form. Given that the binding/releasing of $Ca^{2+}$ at the N-terminal domain of CaM could regulate the dynamic activation of CaM (*50*), the much lower dissociation rate of $La^{3+}$ from the N-terminal domain of CaM could alter such dynamic processes. In addition, the slower dissociation rate of Mas from $La^{3+}$-containing CaM−Mas complexes than that from CaCaM−Mas suggests that in the presence of $La^{3+}$ the durations of the activated CaM as well as the activated CaMBP may be extended. This may be a possible way for $La^{3+}$ to take part in the $Ca^{2+}$-CaM dependent pathway. It was reported previously that the intracellular $La^{3+}$ could be a potent agonist of $Ca^{2+}$-dependent release of catecholamine and histamine (*41*, *51*). There is evidence suggesting that such effects were related to activation of CaM by $La^{3+}$ (*51*). Our present results provide a possible mechanism for these effects.

## CONCLUSION

The present study indicates that $La^{3+}$ shares the same binding sites with $Ca^{2+}$ on CaM. $La^{3+}$ binds to the N-terminal domain of CaM with a slight preference over binding to the C-terminal domain. In the presence of both $Ca^{2+}$ and $La^{3+}$, the hybrid complex $Ca_2La_2CaM$ may form and act as $Ca_4CaM$ in target recognition with a CaM-binding peptide, Mas. The conformations of $Ca_4CaM$ and $La_4CaM$ are different; however, both complexes bind to Mas with similar affinity. In kinetics, the dissociation of $La^{3+}$ from the N-terminal domain of CaM is much slower than that of $Ca^{2+}$, and in $La^{3+}$-containing CaM−Mas ternary complexes, the dissociation rate of Mas is also reduced, indicating that the metal−CaM−Mas ternary complexes become more inert in kinetics in the presence of $La^{3+}$. A possible role of lanthanum ion in the $Ca^{2+}$-CaM-dependent pathway is suggested based on the present results.

## ACKNOWLEDGMENT

Dr. Changwen Jin and Dr. Bing Xia at Beijing NMR Center, Peking University, are gratefully acknowledged for

offering and assisting us to use the Bruker AV 500 NMR spectrometer. We also thank Dr. T. Squier at University of Kansas for the generous gift of the plasmid encoding gene of chicken calmodulin.

## REFERENCES


1. Evans, C. H. (1990) *Biochemistry of Lanthanides*, Plenum Press, New York.
2. Wang, K., Li, R. C., Cheng, Y., and Zhu, B. (1999) Lanthanides—the future drugs? *Coord. Chem. Rev. 190*−*192*, 297−308.
3. Kramsch, D. M., Aspen, A. J., and Rozler, L. J. (1981) Atherosclerosis: Prevention by agents not affecting abnormal levels of blood lipids. *Science 213*, 1511−1512.
4. Sakaida, I., Hironaka, K., Terai, S., and Okita, K. (2003) Gadolinium chloride reverses dimethylnitrosamine (DMN)-induced rat liver fibrosis with increased matrix metalloproteinases (MMPs) of Kupffer cells. *Life Sci. 78*, 943−959.
5. Andres, D., Sanchez-Reus, I., Bautista, M., and Cascales, M. (2003) Depletion of Kupffer cell function by gadolinium chloride attenuates thioacetamide-induced hepatotoxicity. Expression of metallothionein and HSP70. *Biochem. Pharmacol. 66*, 917−926.
6. Ni, J. Z. (2002) *Bioinorganic Chemistry of Rare Earth Elements* (Chinese, 2nd ed.), pp 8−40, Science Press, Beijing.
7. Das, T., Sharma, A., and Talukder, G. (1988) Effects of lanthanum in cellular systems. A review. *Biol. Trace Elem. Res. 18*, 201−228.
8. Greisberg, J. K., Wolf, J. M., Wyman, J., Zou, L., and Terek, R. M. (2001) Gadolinium inhibits thymidine incorporation and induces apoptosis in chondrocytes. *J. Orthop. Res. 19*, 797−801.
9. Praeger, F. C., and Gilchrest, B. A. (1989) Calcium, lanthanum, pyrophosphate, and hydroxyapatite: a comparative study in fibroblast mitogenicity. *Proc. Soc. Exp. Biol. Med. 190*, 28−34.
10. Schorderet-Slatkine, S., Schorderet, M., and Baulieu, E. (1976) Initiation of meiotic maturation in *Xenopus laevis* oocytes by lanthanum. *Nature 262*, 289−290.
11. Smith, J. B., and Smith, L. (1984) Initiation of DNA synthesis in quiescent Swiss 3T3 and 3T6 cells by lanthanum. *Biosci. Rep. 4*, 777−782.
12. Liu, H., Yuan, L., Yang, X., and Wang, K. (2003) $La^{3+}$, $Gd^{3+}$ and $Yb^{3+}$ induced changes in mitochondrial structure, membrane permeability, cytochrome *c* release and intracellular ROS level. *Chem. Biol. Interact.* 146, 27−37.
13. Cheung, W. Y. (1980) Calmodulin plays a pivotal role in cellular regulation. *Science 207*, 19−27.
14. Chin, D., and Means, A. R. (2000) Calmodulin: a prototypical calcium sensor. *Trends Cell Biol. 10*, 322−328.
15. Babu, Y. S., Bugg, C. E., and Cook, W. J. (1988) Structure of calmodulin refined at 2.2 Å resolution. *J. Mol. Biol. 204*, 191−204.
16. Kuboniwa, H., Tjandra, N., Grzesiek, S., Ren, H., Klee, C. B., and Bax, A. (1995) Solution structure of calcium-free calmodulin. *Nat. Struct. Biol. 2*, 768−776.
17. Ikura, M., Clore, G. M., Gronenborn, A. M., Zhu, G., Klee, C. B., and Bax, A. (1992) Solution structure of a calmodulin-target peptide complex by multidimensional NMR. *Science 256*, 632−638.
18. Wang, C. L. (1985) A note on $Ca^{2+}$ binding to calmodulin. *Biochem. Biophys. Res. Commun. 130*, 426−430.
19. Murase, T., and Iio, T. (2002) Static and kinetic studies of complex formations between calmodulin and mastoparanX. *Biochemistry 41*, 1618−1629.
20. Peersen, O. B., Madsen, T. S., and Falke, J. J. (1997) Intermolecular tuning of calmodulin by target peptides and proteins: differential effects on $Ca^{2+}$ binding and implications for kinase activation. *Protein Sci. 6*, 794−807.
21. Bruno, J., Horrocks, W. D., Jr., and Zauhar, R. J. (1992) Europium(III) luminescence and tyrosine to terbium(III) energy-transfer studies of invertebrate (octopus) calmodulin. *Biochemistry 31*, 7016−7026.
22. Horrocks, W. D., Jr., and Tingey, J. M. (1988) Time-resolved europium(III) luminescence excitation spectroscopy: characterization of calcium-binding sites of calmodulin. *Biochemistry 27*, 413−419.
23. Wang, C. L., Aquaron, R. R., Leavis, P. C., and Gergely, J. (1982) Metal-binding properties of calmodulin. *Eur. J. Biochem. 124*, 7−12.
24. Bertini, I., Gelis, I., Katsaros, N., Luchinat, C., and Provenzani, A. (2003) Tuning the affinity for lanthanides of calcium binding proteins. *Biochemistry 42*, 8011−8021.
25. Tsai, M. D., Drakenberg, T., Thulin, E., and Forsen, S. (1987) Is the binding of magnesium (II) to calmodulin significant? An investigation by magnesium-25 nuclear magnetic resonance. *Biochemistry 26*, 3635−3643.
26. Ouyang, H., and Vogel, H. J. (1998) Metal ion binding to calmodulin: NMR and fluorescence studies. *Biometals 11*, 213−222.
27. Buccigross, J. M., and Nelson, D. J. (1986) EPR studies show that all lanthanides do not have the same order of binding to calmodulin. *Biochem. Biophys. Res. Commun. 138*, 1243−1249.
28. Bentrop, D., Bertini, I., Cremonini, M. A., Forsen, S., Luchinat, C., and Malmendal, A. (1997) Solution structure of the paramagnetic complex of the N-terminal domain of calmodulin with two $Ce^{3+}$ ions by 1H NMR. *Biochemistry 36*, 11605−11618.
29. Klumpp, S., Kleefeld, G., and Schultz, J. E. (1983) Calcium/calmodulin- regulated guanylate cyclase of the excitable ciliary membrane from Paramecium. Dissociation of calmodulin by $La^{3+}$: calmodulin specificity and properties of the reconstituted guanylate cyclase. *J. Biol. Chem. 258*, 12455−12459.
30. Mazzei, G. J., Qi, D. F., Schatzman, R. C., Raynor, R. L., Turner, R. S., and Kuo, J. F. (1983) Comparative abilities of lanthanide ions $La^{3+}$ and $Tb^{3+}$ to substitute for $Ca^{2+}$ in regulating phospholipid-sensitive $Ca^{2+}$-dependent protein kinase and myosin light chain kinase. *Life Sci. 33*, 119−129.
31. Sotiroudis, T. G. (1986) Lanthanide ions and $Cd^{2+}$ are able to substitute for $Ca^{2+}$ in regulating phosphorylase kinase. *Biochem. Int. 13*, 59−64.
32. Klee, C. B. (1977) Conformational transition accompanying the binding of $Ca^{2+}$ to the protein activator of 3′,5′-cyclic adenosine monophosphate phosphodiesterase. *Biochemistry 16*, 1017−1024.
33. Urbauer, J. L., Short, J. H., Dow, L. K., and Wand, A. J. (1995) Structural analysis of a novel interaction by calmodulin: high-affinity binding of a peptide in the absence of calcium. *Biochemistry 34*, 8099−8109.
34. Ikura, M., Marion, D., Kay, L. E., Shih, H., Krinks, M., Klee, C. B., and Bax, A. (1990) Heteronuclear 3D NMR and isotopic labeling of calmodulin. Towards the complete assignment of the 1H NMR spectrum. *Biochem. Pharmacol 40*, 153−160.
35. Tjandra, N., Kuboniwa, H., Ren, H., and Bax, A. (1995) Solution structure of calcium-free calmodulin. *Eur. J. Biochem. 230*, 1014−1024.
36. Wang, C. L., Leavis, P. C., and Gergely, J. (1984) Kinetic studies show that $Ca^{2+}$ and $Tb^{3+}$ have different binding preferences toward the four $Ca^{2+}$-binding sites of calmodulin. *Biochemistry 23*, 6410−6415.
37. Bayley, P., Ahlstrom, P., Martin, S. R., Forsen, S. (1984) The kinetics of calcium binding to calmodulin: Quin 2 and ANS stopped-flow fluorescence studies. *Biochem. Biophys. Res. Commun. 120*, 185−191.
38. Brown, S. E., Martin, S. R., and Bayley, P. M. (1997) Kinetic control of the dissociation pathway of calmodulin-peptide complexes. *J. Biol. Chem. 272*, 3389−3397.
39. Malencik, D. A., and Anderson, S. R. (1983) High affinity binding of the mastoparans by calmodulin. *Biochem. Biophys. Res. Commun. 114*, 50−56.
40. Du, X. L., Zhang, T. L., Yuan, L., Zhao, Y. Y., Li, R. C., Wang, K., Yan, S. C., Zhang, L., Sun, H., and Qian, Z. M. (2002) Complexation of ytterbium to human transferrin and its uptake by K562 cells. *Eur. J. Biochem. 269*, 6082−6090
41. Powis, D. A., Clark, C. L., and O'Brien, K. J. (1994) Lanthanum can be transported by the sodium−calcium exchange pathway and directly triggers catecholamine release from bovine chromaffin cells. *Cell Calcium 16*, 377−390.
42. Lansman, J. B. (1990) Blockade of current through single calcium channels by trivalent lanthanide cations. Effect of ionic radius on the rates of ion entry and exit. *J. Gen. Physiol. 95*, 679−696.
43. Cheng, Y., Huo, Q., Lu, J., Li, R., and Wang, K. (1999) The transport kinetics of lanthanide species in a single erythrocyte probed by confocal laser scanning microscopy. *J. Biol. Inorg. Chem. 4*, 447−456.
44. Roland, C. R., Naziruddin, B., Mohanakumar, T., and Flye, M. W. (1996) Gadolinium chloride inhibits Kupffer cell nitric oxide synthase (iNOS) induction. *J. Leukocyte Biol. 60*, 487−492.

45. Spencer, A. J., Wilson, S. A., Batchelor J., Reid A., Rees J., and Harpur E. (1997) Gadolinium chloride toxicity in the rat. *Toxicol. Pathol. 25*, 245−255.
46. Pillai, S., and Bikle, D. D. (1992) Lanthanum influx into cultured human keratinocytes: effect on calcium flux and terminal differentiation. *J. Cell Physiol. 151*, 623−629.
47. Peeters, G. A., Kohmoto, O., and Barry, W. H. (1989) Detection of La3+ influx in ventricular cells by indo-1 fluorescence. *Am. J. Physiol.* 256, C351−C357.
48. Buccigross, J. M., Carey, L. O., and Donald, J. N. (1986) A flow-dialysis method for obtaining relative measures of association cinstants in calmodulin-metal-ion systems. *Biochem. J.* 235, 677−684.
49. Bayley, P. M., Findlay, W. A., and Martin, S. R. (1996) Target recognition by calmodulin: dissecting the kinetics and affinity of interaction using short peptide sequences. *Protein Sci. 5*, 1215−1228.
50. Persechini, A., White, H. D., and Gansz, K. J. (1996) Different mechanisms for $Ca^{2+}$ dissociation from complexes of calmodulin with nitric oxide synthase or myosin light chain kinase. *J. Biol. Chem. 271*, 62−67.
51. Amellal, M., and Landry, Y. (1983) Lanthanides are transported by ionophore A23187 and mimic calcium in the histamine secretion process. *Br. J. Pharmacol. 80*, 365−370.

BI035784I